



Imaging cellular immunotherapies and immune cell biomarkers: from preclinical studies to patients

Alessia Volpe ¹, Prasad S Adusumilli,^{2,3,4} Heiko Schöder,¹ Vladimir Ponomarev ^{1,4,5}

To cite: Volpe A, Adusumilli PS, Schöder H, *et al.* Imaging cellular immunotherapies and immune cell biomarkers: from preclinical studies to patients. *Journal for ImmunoTherapy of Cancer* 2022;**10**:e004902. doi:10.1136/jitc-2022-004902

Accepted 23 July 2022

ABSTRACT

Cellular immunotherapies have emerged as a successful therapeutic approach to fight a wide range of human diseases, including cancer. However, responses are limited to few patients and tumor types. An in-depth understanding of the complexity and dynamics of cellular immunotherapeutics, including what is behind their success and failure in a patient, the role of other immune cell types and molecular biomarkers in determining a response, is now paramount. As the cellular immunotherapy arsenal expands, whole-body non-invasive molecular imaging can shed a light on their *in vivo* fate and contribute to the reliable assessment of treatment outcome and prediction of therapeutic response. In this review, we outline the non-invasive strategies that can be tailored toward the molecular imaging of cellular immunotherapies and immune-related components, with a focus on those that have been extensively tested preclinically and are currently under clinical development or have already entered the clinical trial phase. We also provide a critical appraisal on the current role and consolidation of molecular imaging into clinical practice.

MOLECULAR IMAGING OF T CELL-BASED IMMUNOTHERAPY

Adoptive T cell therapy seeks to harness a patient's immune system to hunt down and kill cancer cells. This new class of 'living drugs' includes tumor-infiltrating lymphocytes (TILs), transgenic endogenous T cell receptor (TCR)-T cells, chimeric antigen receptor (CAR)-T cells and regulatory T cells (Tregs) among others.

Distribution, successful targeting, expansion, infiltration, and antitumor activity are only some of the many aspects influencing the way patients respond to immunotherapy. Answering the following questions might help us improve the safety and efficacy of cell-based immunotherapy:

1. What are the immune cell types contributing to enhance immunotherapy response?
2. Can we identify and monitor a specific subset of T cells?
3. What are the kinetics of distribution of cell-based immunotherapies in the human

body and are they capable to successfully target the tumor?

4. What is their activation status at the tumor site?
5. How long do they persist in the tumor and how does persistence correlate with antitumor response?
6. Do therapeutic cells continue to expand over time and retain their function?
7. What are the factors responsible for the heterogeneous response in patients, and can we predict them?
8. Can we reliably predict and prevent side effects associated with immunotherapy (including on-target off-tumor toxicity, neurotoxicity and cytokine release syndrome (CRS)) in patients?

Non-invasive molecular imaging is a powerful tool that can be successfully employed by scientists and clinicians to answer all above questions and better understand the reasons behind immunotherapy success and, more importantly, its failure. The variety of labeling methods and imaging modalities available can be tailored toward the different types of cellular immunotherapies ([figure 1A](#)), immune-related components (metabolism, checkpoints, etc.) and immune cell biomarkers. In this review, we provide an extensive description of all available modalities and labeling strategies suitable for imaging the immunotherapy paradigm and describe their preclinical and clinical application. Priority has been given to clinically relevant seminal studies.

IMMUNE CELL IMAGING LABELING STRATEGIES AND MODALITIES

Non-invasive molecular imaging of cell-based immunotherapy can be achieved using direct or indirect strategies (refer to Kircher *et al* for graphical representation).^{1,2}



© Author(s) (or their employer(s)) 2022. Re-use permitted under CC BY-NC. No commercial re-use. See rights and permissions. Published by BMJ.

¹Department of Radiology, Memorial Sloan Kettering Cancer Center, New York, New York, USA

²Thoracic Service, Department of Surgery, Memorial Sloan Kettering Cancer Center, New York, New York, USA

³Cellular Therapeutics Center, Department of Medicine, Memorial Sloan Kettering Cancer Center, New York, New York, USA

⁴Center for Cell Engineering, Memorial Sloan Kettering Cancer Center, New York, New York, USA

⁵Molecular Pharmacology and Chemistry Program, Memorial Sloan Kettering Cancer Center, New York, New York, USA

Correspondence to

Dr Vladimir Ponomarev; ponomarv@mskcc.org

Direct cell labeling is based on the *ex vivo* labeling of cells prior to administration into the desired recipient (animal model and/or human) and is particularly used in the context of nuclear-based imaging (positron emission tomography (PET) and single photon emission computed tomography (SPECT)). This approach enables a straightforward labeling of any immune cell or immune-related component but also comes with multiple drawbacks, including label efflux and dilution during cell expansion. With efflux, the probe leaks out of the cell and redistributes throughout the body, rendering it impossible to discriminate between labeled cells and free probe. As the directly labeled cells continue to actively divide, the label is distributed to the progeny and progressively diluted, making it unsuitable to image highly proliferative cells (*e.g.*, T cells). After their systemic administration, pre-labeled T cells generate a detectable signal regardless of their viability status: in fact, damaged and dead cells still lead to signal, resulting in the potential misinterpretation of the patient's response to immunotherapy.

Indirect cell labeling is a very powerful approach for the non-invasive and repetitive observation of T cell-based immunotherapies and is achieved by ectopic expression of a reporter gene in the cell of interest. For details on historical development and reporter expression cassettes refer to Serganova *et al.*³ Foreign or synthetic (non-human derived) reporters are more suited for the *in vivo* highly sensitive monitoring of systemically infused adoptive T cells as they are exclusively expressed in the cells of interest and do not generate background. However, host reporters have the advantage of not eliciting a host immune response. Unlike direct labeling, expression and function of the reporter are strictly linked and are a prerequisite of viable cells, meaning that only intact/healthy cells will result in signal. The permanent integration of the reporter into the host cell genome results in absence of label dilution during cell division and allows the long-term imaging of the rapidly expanding immune cell therapeutics in preclinical models as well as the human body. For preclinical studies, the unlimited imaging window allows to quantify the object of interest without having to sacrifice the animal, thereby significantly reducing the number of animals needed in the study and minimizing the inter-animal variability.

Available imaging strategies that can be tailored toward immunotherapy include: (1) optical, (2) ultrasound (US), (3) MR and (4) nuclear-based imaging. Magnetic particle imaging is an emerging modality in the field of cellular immunotherapies⁴ and will not be discussed in this review.

Optical imaging (OI) is a non-invasive imaging modality using visible, ultraviolet and infrared light and the special properties of photons to acquire biological information. Within this class, fluorescence (FLI) and bioluminescence imaging (BLI) have emerged as powerful modalities. FLI relies on the use of light-activated fluorescent molecules and encompasses a wide range of resolution and imaging depths, from subcellular (<400 μm with

intravital microscopy) to small-animal imaging (1–3 mm spatial resolution at <10 cm with FLI mediated tomography).⁵ FLI reporters are categorized as artificial cell surface molecules, near-infrared, photoactivatable and photoconvertible and (monomeric and non) fluorescent proteins (previously reviewed by Volpe *et al.*)⁶ In BLI, visible light is emitted when an enzyme (*eg.*, a luciferase) oxidizes its own substrate. The enzyme is introduced in the desired cells by genetic engineering and serves as a reporter. Available luciferase enzymes (either present in nature or chimeras) and substrates can be found in a review by Mezzanotte *et al.*⁷

Consideration on optical imaging. BLI and FLI are widely used to track cell-based immunotherapies in preclinical research due to the simplicity of the technique and the affordable costs. Since they do not involve exposure to ionizing radiation, they can be safely used for repeated imaging of immune cells. However, their application to humans is restricted by several key limitations: (1) reporters are typically of non-human origin, thus posing the risk for immunogenicity; (2) limited light tissue penetration; (3) only a qualitative output signal (relative quantification) can be obtained, while other imaging modalities (*e.g.*, positron emission tomography (PET) allow for absolute quantification.

Ultrasound imaging (US) is based on the propagation of mechanical waves from a transducer into the tissue, resulting in echoes that can be resolved to depict objects of interest. US signal is effectively and safely enhanced by contrast agents (encapsulated gas microbubbles or non-microbubbles).

Considerations on ultrasound imaging. US is widely available in preclinical and clinical/diagnostic settings, non-invasive, quantitative and inexpensive compared with other imaging modalities. Depending on the trafficking kinetics of the therapeutic cells, the high temporal resolution of US and fast distribution of contrast agents allows to *in vivo* track them within minutes after probe administration. The rapid clearance also allows the repetitive injection of the agent without having to wait hours or days, although there may not be clinical benefit of doing so in the context of immunotherapy as no significant changes are expected in such a short time. Importantly, with the expansion of the so-called 'acoustogenetics', acoustic reporters may not only be used to non-invasively monitor immune therapeutics, but also to remotely control them for therapeutic purposes.⁸ However, despite the recent development of mammalian-compatible reporters,⁹ the current unavailability of non-immunogenic reporters is limiting their clinical translation.

Magnetic resonance imaging (MRI) excels in soft tissue contrast and not involving ionizing radiation. In fact, it is based on the perturbation of the nuclear magnetic moment of endogenous nuclei (¹H in H₂O) in a magnetic field. Negative contrast agents (iron-oxide nanoparticles)¹⁰ and reporter genes¹¹ result in the reduction or absence of signal. Paramagnetic agents (*eg.*, gadolinium) are positive contrast agents and increase the MRI signal.

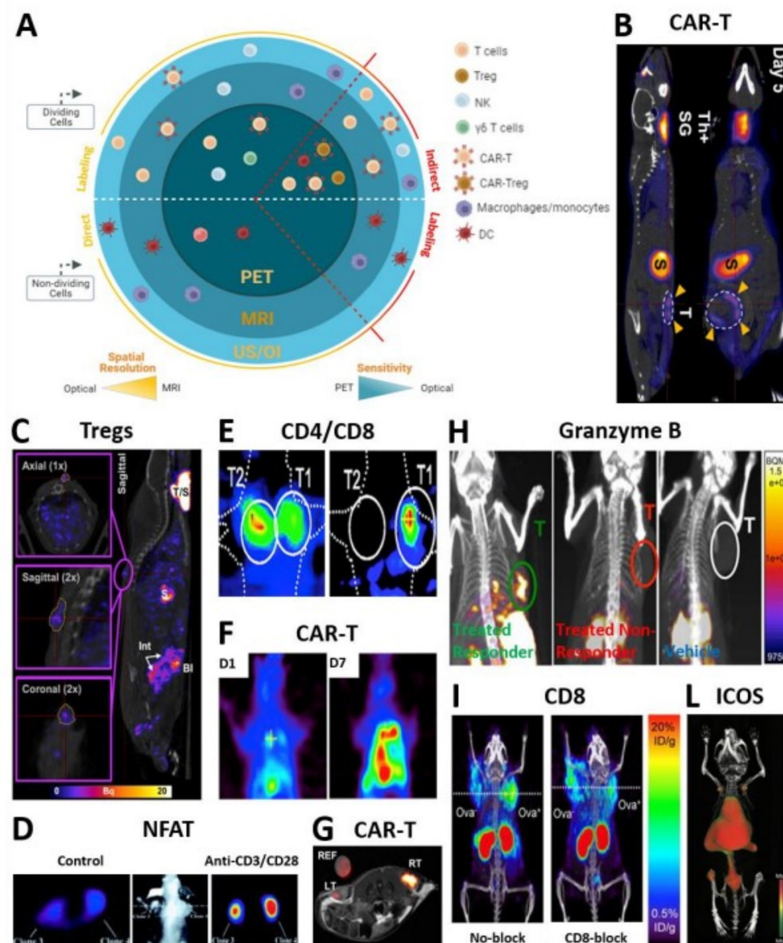


Figure 1 Molecular imaging of cellular immunotherapies and immune-related biomarkers. | T cell trafficking and activation status and biomarkers visualized by different reporter-based and direct imaging modalities. (A) Sketch summarizing all immune cells amenable to molecular imaging through indirect and direct approaches. (B) Coronal and sagittal slices showing intra-tumorally injected panErbB-directed CAR-T cells tumor targeting and retention in a TNBC model by NIS/[¹⁸F]BF₄⁻ PET-CT 5 days post treatment.²⁷ Indicated with yellow arrows are CAR-T cells residing at the tumor. Other signal is due to the endogenous NIS expression: ThSG is thyroid+salivary glands; S is stomach. (C) *In vivo* trafficking and persistence at the skin graft of intravenously administered polyclonal Tregs by NIS/^{99m}TcO₄⁻ SPECT-CT.³³ The sagittal image depicts a representative animal receiving 5 × 10⁶ hNIS-GFP+Tregs 30 days prior to imaging and residing at the skin graft. (D) Transaxial sections show a representative nude mouse bearing different subcutaneously injected Jurkat cells. The NFAT-mediated TKGFP+reporter responded to TCR activation by intravenous administration of anti-CD3/CD28 antibodies (right) as compared with anti-mouse control antibody (left).⁴³ To allow for tracer clearance from the bloodstream and improve signal-to-noise ratio, HSV1-tk/[¹²⁴I] FIAU PET imaging was performed 24 hours post tracer administration. (E) Visualized is selective accumulation of systemically administered EBV-directed CD8+cells in HLA-A0201+EBV BLCL tumor (T1) by HSV1-tk/[¹²⁴I]FIAU PET (right). Although hNET/[¹²³I]MIBG SPECT images show a high accumulation of CD4+cells in corresponding HLA-DRB₁0701+EBV BLCL (T2) tumors (left), signal is detected also in T1 tumor (right), likely caused by the [¹²⁴I]FIAU decay.²² Images were taken 4 hours post administration of a mixture of tracers. (F) [¹⁸F]-FEAU PET showing increased intrapleural accumulation of HSV-tk+mesothelin-targeted CAR-T cells by day seven post regional infusion in an orthotopic model of fLuc+mesothelioma.⁷⁴ The latter correlated to decreased tumor burden as depicted by tumor BLI (not shown). (G) TATP-F68-PFC labeled 1 × 10⁷ human CAR-T cells visualized by *in vivo* ¹⁹F MRI (RT: right tumor) as compared with F68-PFC control (LT: left tumor) in a mouse glioma model.⁷⁵ ¹⁹F image of injected cells is in pseudo-color; T₂-weighted ¹H image of tumors is in greyscale. (H) anti PD-1 and anti-CTLA-4 immunotherapy efficacy assessed 12 days post treatment by *in vivo* imaging of granzyme B as a marker of T cell activation using ⁶⁸Ga-NOTA-GZP probe for PET-CT.⁴¹ Sagittal images showing differentiation between responders treated (green), non-responders treated (red) and vehicle treated (white) mice. (I) Representative PET-CT images acquired 22 hours post ⁸⁹Zr-malDFO-169 cystidiobody injection and showing unblocked and CD8-blocked mice bearing EL4-Ova⁻ (left) and EL4 Ova⁺ (right) tumors 5 days postadoptive OT-I T cell transfer.³⁸ (L) Coronal-ventral view of CD-19-targeted CAR-T cell activation during anti-tumor response by ⁸⁹Zr-DFO-ICOS mAb PET-CT. Signal due to successful targeting is detected in lumbar vertebrae, iliac bone, femur and tibia. Signal due to tracer clearance is in heart, spleen and liver. imaging performed 5 days post-CAR-T cell systemic delivery and 48 hours post-tracer administration.⁷⁶ All figures adapted with permission from publishers. DC, dendritic cell; hNIS, human sodium iodide symporter; NFAT, nuclear factor of activated T cells; PET, positron emission tomography; SPECT, single photon emission computed tomography; TCR, T cell receptor; TNBC, triple-negative breast cancer.

Considerations on magnetic resonance imaging. Magnetic nanoparticles and reporter genes can be both used to label cell-based immunotherapies. Positive contrast agents are not safe and sensitive enough to be clinically translated.¹² Different chemical exchange saturation transfer MRI approaches have been developed to image T cell metabolites changes as biomarkers of their activation state and response to immunotherapy.¹³

Nuclear-based imaging offers whole-body non-invasive imaging capabilities for preclinical and clinical application.¹⁴ Direct labeling can be performed using SPECT-compatible and PET-compatible radioactive probes, while the indirect labeling is based on cell engineering with foreign, host and synthetic radionuclide-based reporter genes. The reporter transgene can encode for: (1) transporters (internalizing the probe), (2) receptors (expressed on the plasma membrane of cells and irreversibly binding to the probe) or (3) enzymes (modifying the probe structure and resulting in its entrapment and intracellular accumulation). For a complete list of available nuclear-based reporters and paired probes refer to Volpe *et al.*¹⁴

Consideration on nuclear-based imaging. In addition to the already discussed limitations of direct labeling, a few more considerations are needed. As the overall signal strength of directly labeled cells is only retained until radiotracer decay, the choice of tracers with longer half-life is crucial to extend the already limited time window for imaging. However, this approach would have consequences for the management of patients and their body excreta, thus posing a limitation for its clinical translation. Moreover, the longer decay prolongs the time of radioactivity emission in the patient's body and may, therefore, damage the healthy tissues and impact on the viability of the labeled immune cells. In fact, clinically used radiotracers (*e.g.*, ¹¹¹In-oxine, ⁸⁹Zr-oxine), when used at high concentrations, can interfere with cell survival and proliferative ability.¹⁵ On the other hand, reporter-based imaging of cellular immunotherapies is not dictated or limited by the radiotracer half-life. In fact, short-lived isotopes are not only used but also recommended to avoid potential toxicity and radio-damage of target cells. However, challenges posed to the strategy include (1) potential immunogenicity of foreign and/or synthetic reporters, (2) elaborate and costly protocols, (3) access to highly skilled research personnel to conduct cell engineering, *in vitro* assays, development of mouse models and often long and elaborate *in vivo* imaging experiments and (4) the need of a solid imaging infrastructure and annexed radiochemistry facility.

Application of imaging toward cell-based immunotherapy

Conventional imaging methodologies routinely used in clinical practice focus on assessment of disease response by providing anatomic (*e.g.*, computed tomography (CT), MRI) or metabolic (*e.g.*, [¹⁸F]-fluorodeoxyglucose (FDG)-PET, functional MRI) information of the tumor but fail to give a complete representation of the complex

spectrum of responses to immunotherapy. As the latter is often accompanied by an initial 'pseudoprogression', understanding the distinctive features of tumors treated with immunotherapy and the fate of these 'living drugs' is paramount to reliably predict responses.

Here we report seminal studies using molecular imaging for the non-invasive preclinical and clinical imaging (tables 1 and 2) of cellular immunotherapies and immune biomarkers, searched using "immunotherapy", "cancer", and "imaging" key words and by literature search on PubMed.

Imaging T cell trafficking and persistence

Current clinical trials involving infusion of cell-based immunotherapies are performed without knowledge of their whole-body distribution during treatment. Cell-based therapeutics can potentially redistribute and lead to so-called 'on-target off-site' toxicity, causing severe side effects or even death. Non-invasive long-term imaging can be used for the monitoring of their spatiotemporal *in vivo* distribution, persistence at the tumor site, survival and *in situ* expansion.

Cytolytic T cells (CTLs). Nuclear imaging with FDA-approved ¹¹¹In-oxine clinical probe¹⁶ and ⁸⁹Zr-oxine¹⁵ was employed to track the fate of directly labeled CTLs. A good manufacturing practise (GMP)-compatible production of ⁸⁹Zr-oxine and white blood cell radiolabeling has been described and could accelerate its application in in-human cell imaging studies.¹⁷ Indirect strategies for *in vivo* tracking of T cells involve the use of BLI (overviews from Costa *et al.*¹⁸ and Rabinovich *et al.*¹⁹) or nuclear-based (overview from Volpe *et al.*) reporters.¹⁴ Koehne *et al.* demonstrated for the first time the feasibility of long-term imaging of CTLs by HSV1-tk/[¹³¹I]FIAU- and [¹²⁴I]FIAU-PET.²⁰ As the interplay between CD4+ and CD8+ T cells has a significant impact on the kinetics, persistence and antitumor activity of adoptive cell therapies,²¹ a reporter-based method was developed preclinically to independently track the CD4+ and CD8+ T cells by human norepinephrine transporter (hNET)-afforded -SPECT and HSV1-tk-afforded-PET, respectively (figure 1E).²² Notably, a human carcinoembryonic antigen (hCEA) reporter could also be used for the molecular imaging of adoptive T cell therapies, provided that the target tissue is not expressing any hCEA.²³

Chimeric antigen receptor (CAR)-T cells. Direct labeling protocols using ⁸⁹Zr-oxine²⁴ and ⁸⁹Zr-DFO²⁵ have been developed for the *in vivo* tracking of CAR-T cells. Many host, foreign and synthetic reporter genes were also employed and provided a greater advantage for the repeated monitoring of CAR-T cells by either optical, ultrasound, nuclear imaging or hybrid. Moroz *et al.* preclinically demonstrated the superiority of hNET/[¹⁸F]MFBG reporter/probe combination for the repeated imaging of T cells (sensitivity of 1×10^5 T cells/cm³).²⁶ CAR-T detection sensitivity was as high as 3000 cells with sodium iodide symporter (NIS)-based [¹⁸F]BF₄-PET (figure 1B) and revealed the inverse correlation

Table 1 Seminal preclinical nuclear-based, MRI and ultrasound studies employing direct and indirect molecular imaging for the *in vivo* monitoring of T cell-based immunotherapies and their immune-related components

Immune Cell	Molecular Target	Imaging agent	Labeling approach	Reporter Gene	Imaging modality	Ref
T lymphocyte	n/a	⁸⁹ Zr-oxine	Direct	n/a	PET	15
T lymphocyte	n/a	¹¹¹ In-oxine	Direct	n/a	SPECT	16
T lymphocyte	n/a	¹⁸ F]MFBG and (¹²³ I/ ¹²⁴ I)MIBG, ¹²⁴ I, ¹⁸ F-FAU, ¹²⁴ I-FAU	Indirect	hNET, hNIS, dCKDM, HSV1- <i>tk</i>	PET	26
T lymphocyte	n/a	¹²⁴ I scFv antibody fragment	Indirect	CEA N-A3	PET	23
T lymphocyte	n/a	¹²⁴ I-FAU	Indirect	HSV1- <i>tk</i> , GFP	PET	43
T lymphocyte	Pan-ErbB CAR	(¹⁸ F)BF ₄ ⁻	Indirect	hNIS	PET	27
T lymphocyte	CD19 CAR	(¹⁸ F)DCFPYL	Indirect	tPSMA ^(N9del)	PET	28
T lymphocyte	GD2 CAR	(¹⁸ F)TMP	Indirect	eDHFR	PET	29
T lymphocyte	CD19 CAR	⁸⁶ Y-AAABD	Indirect	DAbR1	PET	30
T lymphocyte	EGFRvIII CAR	¹⁹ F-PFC	Direct	n/a	MRI	75
T lymphocyte	CD19 CAR	n/a	Indirect	Heat-inducible-GFP-PGK-mCherry	MRI-guided FUS	8
T lymphocyte	OX40	⁶⁴ Cu-DOTA-ABox40	Direct	n/a	PET	77
T lymphocyte	ICOS	⁸⁹ Zr-DFO-ICOS	Direct	n/a	PET	76
T lymphocyte	IL-2	(¹⁸ F)FB-IL-2	Direct	n/a	PET	78
T lymphocyte	TCR	⁶⁴ Cu-DOTA-KJ1-26	Direct	n/a	PET	79
T lymphocyte	CD3	⁸⁹ Zr-DFO-CD3	Direct	n/a	PET	80,81
T lymphocyte	CD4	⁸⁹ Zr-GK1.5 cDb	Direct	n/a	PET	82
T lymphocyte	CD8	⁸⁹ Zr- maIDFO-169 cDb and ⁶⁴ Cu-169 cDb	Direct	n/a	PET	38,83
T lymphocyte	CD4/CD8	(¹²³ I)MIBG/(¹²⁴ I)FAU	Indirect	hNET/ HSV1- <i>tk</i>	SPECT/ PET	22
T lymphocyte	CD8	SPIO	Direct	n/a	MRI	84
T lymphocyte	Granzyme B	⁸⁸ Ga-NOTA-GZP	Direct	n/a	PET	41
T lymphocyte	IFN- γ	⁸⁹ Zr- IFN- γ	Direct	n/a	PET	42
T lymphocyte	n/a (phosphorylated by TK _i)	(¹⁸ F)FLT	Direct	n/a	PET	54,62
T lymphocyte	dGK	(¹⁸ F)F-AraG	Direct	n/a	PET	85
T lymphocyte	dCK	(¹⁸ F)CFA/(¹⁸ F)FAC/(¹⁸ F)FACB	Direct	n/a	PET	86,87
T lymphocyte	PD-1	⁶⁴ Cu- PD-1, ⁶⁴ Cu-DOTA- PD-1, ⁶⁴ Cu-NOTA-PD-1, ⁸⁹ Zr-Df-Pembrolizumab, ⁸⁹ Zr-Df-Nivolumab	Direct	n/a	PET	47,48,88,89

Continued

Table 1 Continued

Immune Cell	Molecular Target	Imaging agent	Labeling approach	Reporter Gene	Imaging modality	Ref
T lymphocyte	PD-L1	^{99m} Tc, ¹¹¹ In, ¹¹¹ In-DTPA, ⁸⁹ Zr-DFO, ⁶⁴ Cu, ⁶⁴ Cu-DOTA, ⁶⁸ Ga-NOTA, ¹⁸ F-BMS-986192	Direct	n/a	SPECT/PET	36,46,50,51
T lymphocyte	CTLA-4	⁶⁴ Cu-DOTA- and NOTA-Ipilimumab	Direct	n/a	PET	52,53
T lymphocyte	LAG-3	^{99m} Tc, ⁸⁹ Zr-REGN3767	Direct	n/a	SPECT, PET	55,56
T lymphocyte	TIM-3	⁶⁴ Cu-NOTA-RTM3-23	Direct	n/a	PET	57
T lymphocyte	TIGIT	⁸⁹ Zr- and ⁶⁴ Cu-AB154	Direct	n/a	PET	58
Treg	n/a	^{99m} TcO ₄ ⁻	Indirect	hNIS	SPECT	33
Treg	IL-10-HLA-A2 CAR	^{99m} TcO ₄ ⁻	Indirect	hNIS	SPECT	34
Gamma delta T lymphocyte	n/a	⁸⁹ Zr-oxine	Direct	n/a	PET	35
NK	n/a	⁸⁹ Zr-oxine	Direct	n/a	PET	60
NK	n/a	(¹⁸ F)FDG	Direct	n/a	PET	59
NK	n/a	¹⁹ F-PFC, ¹⁹ F, Ferumoxides/Ferucarbotran	Direct	n/a	MRI	59
DC	n/a	(¹⁸ F)BF ₄ ⁻	Indirect	hNIS	PET	65
DC	n/a (phosphorylated by TK _i)	(¹⁸ F)FLT	Direct	n/a	PET	62
DC	n/a	¹⁹ F-PFC, ¹⁹ F, SPIO	Direct	n/a	MRI	61,64
DC	n/a	n/a	Indirect	Ferritin	MRI	66
Macrophages	n/a	SPION ferumoxytol	Direct	n/a	MRI	67
Monocytes/macrophages	CD40	⁸⁹ Zr-TRAF6i-HDL	Direct	n/a	PET	90
Monocytes	n/a	¹⁹ F-PFC	Direct	n/a	MRI	68

BI, Boehringer Ingelheim; BMS, Bristol-Myers Squibb; CAR, chimeric antigen receptor; CEA, carcinoembryonic antigen; DC, dendritic cell; dCK, Deoxycytidine kinase; Df or DFO, Deferoxamine; dGK, Deoxyguanosine; DOTA, 1,4,7,10-Tetraazacyclododecane-1,4,7,10-tetraacetic acid; eDHR, *Escherichia Coli* dihydrofolate reductase; EGFRvIII, Epidermal Growth Factor Receptor variant III; [¹⁸F]BF₄⁻, Tetrafluoroborate; [¹⁸F]CFA, [¹⁸F]Clorafabine; [¹⁸F]DCCFPyL, Pflufolastat fluorine ¹⁸F; [¹⁸F]FAC, 1-(2'-deoxy-2'-F-fluoroarabino-furanosyl) cytosine; [¹⁸F]F-AraG, 2'-deoxy-2'-[¹⁸F]-fluoro-9β-D-arabino-furanosyl-guanine; [¹⁸F]FBB-IL-2, N-(4-¹⁸F-fluorobenzoyl)-interleukin-2; [¹⁸F]FDG, [¹⁸F]fluorodeoxyglucose; [¹⁸F]FHBG, 9-(4-(18F)-Fluoro 3(hydroxymethyl)butyl)guanine; [¹⁸F]FIAU, 2'-deoxy-2'-[¹⁸F]-fluoro-1-beta-D-arabino-furanosyl-5-iodouracil; [¹⁸F]FLT, [¹⁸F]flutrothymidine; (¹⁸F)TMP, (¹⁸F)fluoropropyl-trimethoprim; FUS, Focused Ultrasound; ⁶⁸Ga-NOTA-HGZF, ⁶⁸Gallium-1,4,7-Triazacyclononane-1,4,7-triacetic acid-human biotin βAla-GGG-IEPD-CHO; GRM13Z40, Interleukin-13 zetakine Receptor Alpha 2-targeted CAR; hNET, human norepinephrine transporter; hNIS, human sodium iodide symporter; [²⁴]FIAU, [²⁴]FIAU, [¹²⁴I]-2'-fluoro-deoxy-1-beta-D-arabino-furanosyl-5-iodouracil; [¹²⁵I]MIBG, [¹²⁵I]metaiodobenzylguanidine; n/a, not available; NK, natural killer; PET, positron emission tomography; PFC, Perfluorocarbon; P28z, PSMA-targeted CD28z CAR; SPECT, single photon emission computed tomography; SPION, superparamagnetic iron oxide nanoparticle; TRAF6, tumor necrosis factor receptor-associated factor 6; ⁸⁹Y-AABD, ⁸⁹yttrium (S)-2-(4-acrylamidobenzyl)-DOTA.

Table 2 Past and ongoing clinical trials with their respective molecular targets and imaging agents used for the nuclear-based and MRI-based imaging of T cell-based immunotherapy and related immune components

Molecular target	Imaging Agent	Labeling approach	Imaging modality	ClinicalTrial.gov identification	Status	Ref.
IL-2	(¹⁸ F)FB-IL-2	Direct	PET	NCT02922283	Terminated, no correlation	37
IL-2	^{99m} Tc-HYNIC-IL-2	Direct	PET	NCT01789827	Completed	91
CD8	⁸⁹ Zr-Df-IAB22M2C	Direct	PET	NCT03802123, NCT03107663	Active (not recruiting), Completed	39
CD8	⁸⁹ Zr-ZED88082A	Direct	PET	NCT04029181	Recruiting	92
CD8	⁸⁹ Zr-DFO-REGN5054	Direct	PET	NCT05259709	Not yet recruiting	40
Granzyme B	⁶⁸ Ga-NOTA-hGZP	Direct	PET	NCT04169321	Recruiting	41
dGK	(¹⁸ F)F-AraG	Direct	PET	NCT03142204, NCT03007719, NCT03129061	Recruiting, Terminated, Recruiting	93
dCK	(¹⁸ F)CFA, (¹⁸ F)FAC	Direct	PET	NCT03409419	Completed	46 94
PD-1	⁸⁹ Zr-Pembrolizumab	Direct	PET	NCT02760225	Completed	49
PD-1	⁸⁹ Zr-Nivolumab	Direct	PET	2015-004760-11	Active	36
PD-L1	¹⁸ F-BMS-986192	Direct	PET	NCT03843515, NCT03520634	Active (not recruiting), Completed	51
PD-L1	⁸⁹ Zr-Durvalumab	Direct	PET	NCT03829007, NCT03610061	Completed, Recruiting	36
PD-L1	⁸⁹ Zr-MEDI4736	Direct	PET	NCT03853187	Recruiting	36
PD-L1	⁸⁹ Zr-Avelumab	Direct	PET	NCT03514719	Completed	36
PD-L1	⁸⁹ Zr-Atezolizumab, ⁸⁹ Zr-MDPL-3280A	Direct	PET	NCT03850028, NCT02453984, NCT02478099	Recruiting, Active (not recruiting), Recruiting	36
PD-L1	⁸⁹ Zr- DFO-REGN3504	Direct	PET	NCT03746704	Recruiting	36
CTLA-4	⁸⁹ Zr-Ipilimumab	Direct	PET	NCT03313323	Recruiting	36
CTLA-4	(¹⁸ F)FLT	Direct	PET	NCT00471887	Completed	54
LAG-3	⁸⁹ Zr-DFO-REGN3767,	Direct	PET	NCT04706715, NCT04566978	Recruiting, Recruiting	36 56
LAG-3	⁸⁹ Zr-BI 754111	Direct	PET	NCT03780725	Terminated	95
TIM-3	(¹⁸ F)CFA	Direct	PET	NCT03409419	Completed	96
HSV1-tk/ GRm13Z40 CAR-T	(¹⁸ F)FHBG	Indirect	PET	NCT00730613, NCT01082926	Completed	31
HSV1-tk/P28z CAR-T	(¹⁸ F)FIAU	Indirect	PET	NCT01140373	Active, not recruiting	97
HSV1-tk/CD34 T cells	(¹⁸ F)FHBG	Indirect	PET	NCT00871702	Completed	98
DC	(¹⁸ F)FLT	Direct	MRI	NCT00243529	Completed, Completed	62
DC	SPIO/ ¹¹¹ In-oxine	Direct	MRI	NCT00243594	Completed	63

BI, Boehringer Ingelheim; BMS, Bristol-Myers Squibb; DC, dendritic cell; dCK, Deoxycytidine kinase; Df or DFO, Deferoxamine; dGK, Deoxyguanosine; [¹⁸F]CFA, [¹⁸F]Clorafabine; [¹⁸F]FAC, 1-(2'-deoxy-2'-¹⁸F-fluoroarabino-furanosyl) cytosine; [¹⁸F]F-AraG, 2'- deoxy-2'-¹⁸F-fluoro-9β-D-arabinofuranosyl-guanine; [¹⁸F]FB-IL-2, N-(4-¹⁸F-fluorobenzoyl_interleukin-2; [¹⁸F]FHBG, 9-(4-(¹⁸F)-Fluoro-3[hydroxymethyl] butyl)guanidine; [¹⁸F]FIAU, 2'-deoxy-2'-[¹⁸F]-fluoro-1-beta-D-arabinofuranosyl-5- iodouracil; ⁶⁸Ga-NOTA-hGZP, ⁶⁸Gallium-1,4,7-Triazacyclononane-1,4,7-triacetic acid-human biotin-βAla-GGG-IEPD-CHO; GRm13Z40, Interleukin-13 zetakine Receptor Alpha 2-targeted CAR; PET, positron emission tomography; P28z, PSMA-targeted CD28z CAR; SPIO, superparamagnetic iron oxide.

between CAR-T tumor retention and PD-L1 expression in triple-negative breast cancer models.²⁷ tPSMA^{N9Del}-based [¹⁸F]DCFPyL PET enabled the reliable detection of 2000 CAR-T cells and the visualization of CAR-T

infiltration into local and metastatic lesions in a model of acute lymphoblastic leukemia.²⁸ A novel reporter, eDHFR, derived from *E. Coli* allowed for successful visualization of GD2-specific CAR-T cells targeting human

colorectal xenografts using [^{18}F]TMP-afforded PET.²⁹ A novel DOTA antibody reporter 1 (DABR1) irreversibly binding to the lanthanoid (*S*)-2-(4-acrylamidobenzyl)-DOTA (AABD) was tested in xenografts and provided information on the *in vivo* distribution and homing of systemically administered CD19-directed CAR-T cells at the tumor using ^{86}Y - and ^{177}Lu -AABD.³⁰ The first

documented in-human study by Keu *et al*³¹ showed the trafficking of CD8+GRm13Z40 (interleukin-13 zeta-kinase receptor alpha 2)-targeted CAR-T cells previously infused into the medial left frontal lobe of patients with high grade glioma, providing insights on their successful homing at the tumor by HSV1-*tk* / [^{18}F]FHBG PET (figure 2A; NCT01082926).³¹

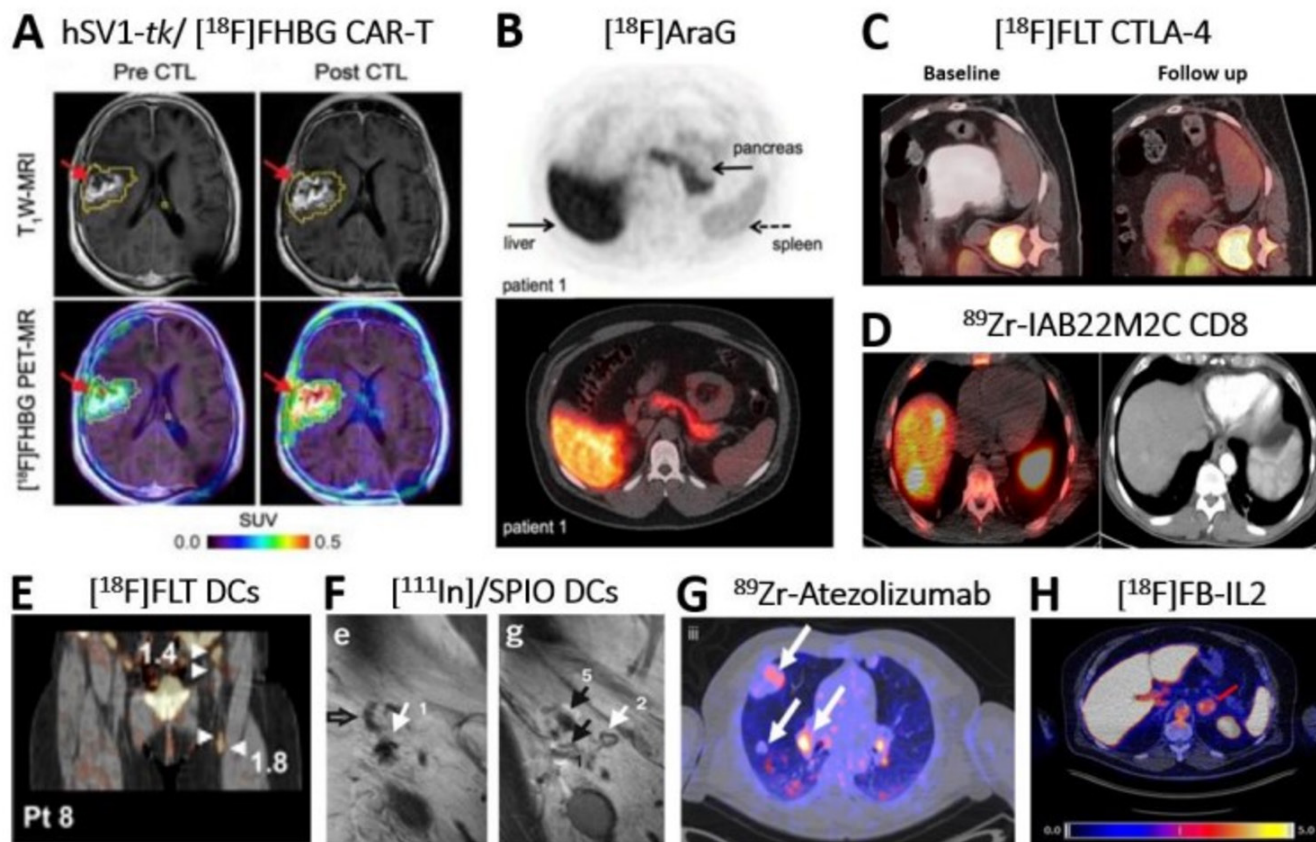


Figure 2 Clinical application of direct and indirect molecular imaging in cell-based Immunotherapy. (A) Non-invasive reporter gene imaging of IL-13 zeta-kinase-directed and HSV1-*tk*-expressing CAR-T cells in a 66-year-old patient with recurrent frontoparietal glioblastoma. [^{18}F]FHBG PET-CT revealed increased uptake after CAR-T cells infusion 1-week post infusion. Tumor extent was assessed by T₁W MRI (top row) before and after CAR-T intratumoral infusion. Images were superimposed with [^{18}F]FHBG PET (bottom row).³¹ (B) Image of a healthy volunteer showing [^{18}F]AraG tracer *in vivo* distribution 60 min post intravenous administration of 189.07 MBq.⁹⁹ The tracer exhibits hepatobiliary and renal clearance. Shown are transversal PET (top) and fused PET-CT (bottom). (C) [^{18}F]FLT PET-CT imaging revealed T cell splenic proliferation in a patient with metastatic melanoma undergoing a durable regression post anti-CTLA-4 (tremelimumab) treatment.⁵⁴ Baseline scan (left) was compared with a 3-month follow-up scan (right). (D) ^{89}Zr -IAB22M2C PET-CT of CD8+T cells performed in a patient with hepatocellular carcinoma on immunotherapy for 12 weeks prior to imaging.^{39,40} Zr-IAB22M2C-positive lesions in the PET-CT merge (left image) correspond to two liver metastases (left side), spleen (right side) and bone marrow (middle). Additional uptake was seen also in three abdominal lymph node metastases. CT alone is in right image. Images acquired 24 hours post tracer injection. (E) [^{18}F]FLT PET-CT visualizes immune responses in four LNs (see arrows) 3 days after intranodal delivery of [^{111}In]/SPIO-labeled and antigen-loaded DCs and 1 hour after tracer injection.⁶² In fact, tracer retention was observed in the injected In and the three draining LNs. (F) *In vivo* migration of [^{111}In]/SPIO-labeled dendritic cells from LN1 (site of injection; arrow 1/e) to other LNs (arrows 5/g) using MRI.⁶³ Open arrow in left image (E) indicates empty In (NO SPIO); closed black arrow in right image (G) indicates In positive for SPIO. Images taken 2 days post intranodal injection of DCs. (G) ^{89}Zr -Atezolizumab PET revealed uptake in different tumor lesions (white arrows) in one representative patient 7 days postinjection.¹⁰⁰ Pronounced uptake heterogeneity was seen within the same patient. (H) [^{18}F]FB-IL2 uptake corresponding to activated tumor-infiltrating T cells at an adrenal gland metastasis (red arrow) in a representative melanoma patient undergoing immune checkpoint inhibitor therapy (SUV_{max} of 5.2).³⁷ All patients enrolled in this study received intravenous bolus injection of ~200 MBq [^{18}F]FB-IL2 in 5 min. Transversal PET-CT image shown. All figures adapted with permission from publishers. CAR, chimeric antigen receptor; DC, dendritic cell; LNs, lymph nodes; SPIO, superparamagnetic iron oxide; PET, positron emission tomography.

Imaging regulatory T cells and gamma delta T cells

Regulatory T cells (Tregs). The efficacy of adoptive regulatory T cells (Treg) therapy (based on either polyclonal or the more potent antigen-specific Tregs), was demonstrated in numerous preclinical disease models and clinical trials.³² Nuclear-based reporter gene imaging offers a clinically compatible platform for future Tregs imaging in humans by providing the missing information on their *in vivo* distribution and persistence and addressing potential safety concerns. Notably, NIS-afforded SPECT-CT allowed tracking of human polyclonal Tregs to the human skin transplant in humanized mice (figure 1C). Authors further demonstrated that Tregs successful trafficking to the skin graft is regulated by Gr-1⁺ neutrophils and monocytes.³³

CAR-Tregs. To improve specificity for the target antigen and therapy success, the field is quickly evolving from polyclonal to CAR-Tregs. As a result, more CARs are being developed and require *in vivo* testing by molecular imaging. Notably, HLA-A2 CAR-Tregs were recently engineered to constitutively express IL-10 and NIS reporter. *In vitro*, cells maintained their phenotype and gained an additional suppressive advantage, while NIS could be used for their non-invasive *in vivo* monitoring.³⁴

Gamma delta T cells. They exert their cytotoxic activity through antigens recognition and indirectly enhance the anti-tumor activity of other immune cells by secreting multiple cytokines. Tracking with ⁸⁹Zr-oxine in a xenograft model of human triple-negative breast cancer revealed a significantly increased tumor infiltration upon pretreatment with PEGylated liposomal alendronate.³⁵

Functional Imaging of T cells

Upon antigen recognition and engagement, T cells upregulate multiple activation biomarkers (surface, nuclear), leading to the release of anti-tumor cytokines. Those are early predictive biomarkers of immunotherapy response, providing valuable information on T cell activation and expansion (*e.g.*, signal increase over time), and can be targeted by molecular imaging.³⁶ Like cancer cells, activated T cells undergo metabolic reprogramming to survive the hostile tumor microenvironment (TME) and retain their antitumor activity. Those metabolic changes can also be *in vivo* monitored in real-time using molecular imaging.

T cell activation biomarkers. *In vivo* imaging of T cell-surface markers (such as the costimulatory molecules OX40 and ICOS (figure 1L), IL-2 (NCT01789827; NCT02922283 in figure 2H),³⁷ TCR and lineage defining molecules (including CD3, CD4, and CD8) was successfully performed using direct labeling with PET radiotracers.³⁶ Preclinical testing of ⁸⁹Zr-DFO anti-CD8 cys-diabody (figure 1I)³⁸ and ⁸⁹Zr-Df-IAB22M2C minibody (figure 2D; trialed in NCT04029181, NCT03107663, NCT03802123)³⁹ revealed CD8⁺T cells response against cancer. A new ⁸⁹Zr-DFO-REGN5054 antibody⁴⁰ for the non-invasive detection of CD8 expression is now in clinical trial (NCT05259709). Other T cell-surface markers

associated with T cell activation, such as PD-1, CTLA-4, TIM-3 and LAG-3, are also immune checkpoint molecules and will be discussed in their dedicated section.

Targets related to T cell activation. Granzyme B is a predictive biomarker of successful checkpoint immunotherapy and can be imaged by ⁶⁸Ga-NOTA-GZP PET (figure 1H; NCT04169321).⁴¹ Similarly, a preclinically tested ⁸⁹Zr-labeled monoclonal antibody targeting IFN-gamma may provide insights on immune T cell activation and function.⁴²

Nuclear Factor of Activated T cells (NFAT)-mediated T cell activation. Ponomarev *et al* described a TCR-dependent NFAT-HSV1-*tk*-GFP inducible PET-FLI dual-reporter system under the control of an artificial *cis*-acting NFAT-specific enhancer (figure 1D).^{43,44} On TCR-MHC complex engagement, the NFAT-HSV1-*tk*-GFP starts reporting on NFAT-mediated transcription of IL-2 and other cytokines, thereby providing information on the *in vivo* activation status of T cells. The combination of NFAT-inducible and constitutive reporters allowed to simultaneously visualize the trafficking, proliferation and activation of donor T cells and T cell precursors during T cell development after allogeneic hematopoietic stem cell transplantation in a mouse model of graft-versus-host disease.⁴⁵

Metabolic targets. [¹⁸F]FDG imaging is routinely used to assess the changes in glucose metabolism and monitor the response in patients undergoing immunotherapy, including checkpoint inhibition.³⁶ Other ¹⁸F-based examples are in overview from van der Veen *et al*.⁴⁶

Imaging the Tumor Microenvironment (TME)

As the TME plays a critical role in immune surveillance and immune evasion, its major regulators can be considered promising immunotherapeutic targets. Immunosuppressive conditions include the upregulation of several immune checkpoints negatively regulating T cell activity (*e.g.*, PD-1/PD-L1, CTLA-4, TIM-3 and LAG-3). Targeting of checkpoints by so-called ‘immune checkpoint inhibitors’ led to the Food and Drug Administration (FDA) approval for clinical use of (1) PD-1 inhibitors (*e.g.*, pembrolizumab, nivolumab), (2) PD-L1 inhibitors (*e.g.*, atezolizumab, avelumab, durvalumab) and (3) CTLA-4 inhibitor (ipilimumab). All immune checkpoints are amenable to molecular imaging and a wide range of agents has already been developed to non-invasively interrogate their heterogeneous expression and dynamics in preclinical models and clinical trials.^{36,46}

Programmed cell death protein 1 (PD-1/CD279). A preclinical evaluation of ⁸⁹Zr-labeled FDA-approved Pembrolizumab (Keytruda; humanized IgG4) suggested its use for the selection of patients benefitting from anti-PD-1 therapy.⁴⁷ Suitability of ⁸⁹Zr-labeled FDA-approved anti-PD-1 antibody Nivolumab as a diagnostic and disease monitoring tool is being investigated in a clinical trial (2015-004760-11).⁴⁸ Accurate identification of early responses and resistance to PD-1 blockade was assessed by ⁸⁹Zr-labeled Pembrolizumab PET (NCT02760225).⁴⁹

Programmed cell death protein ligand 1 (PD-L1/CD274). Antibody-based therapies targeting PD-L1 aim to monitor its *in vivo* expression as a predictive biomarker for checkpoint inhibitor therapy success. Examples are the newly developed nanobodies against PD-L1⁵⁰ and BMS-986192 tracer⁵¹ for SPECT and PET imaging, respectively. The latter tracer is now in two clinical trials (NCT03843515, NCT3520634).

Cytotoxic T lymphocyte-associated protein 4 (CTLA-4/CD152). Imaging CTLA-4 as a predictive biomarker of anti-CTLA-4 therapy is a useful tool. To reliably monitor CTLA-4 *in vivo* expression, the FDA-approved CTLA-4 antibody Ipilimumab was radiolabeled with multiple PET tracers and validated in xenograft⁵² and humanized mouse models.⁵³ In a clinical trial, investigators are studying if high uptake of ⁸⁹Zr-*Ipilimumab* correlates to treatment response (NCT033313323). As CTLA-4 blockade prevents engagement to B7 costimulatory molecules and promotes T cell activation and proliferation, [¹⁸F]FLT PET can detect the associated changes in DNA synthesis during anti-CTLA-4 therapy in secondary lymphoid organs (*e.g.*, spleen) of patients with metastatic melanoma (figure 2C; NCT00471887).⁵⁴

Lymphocyte activation gene 3 protein (LAG-3). The *in vivo* expression of LAG-3 can be assessed using ^{99m}Tc labeled nanobodies⁵⁵ and ⁸⁹Zr labeled REGN3767 fully human anti-LAG-3 antibody.⁵⁶ Clinical studies with ⁸⁹Zr-DFO-REGN3767 are ongoing in patients with diffuse large B-cell lymphoma (NCT04566978) and advanced solid tumors (NCT04706715).

T cell immunoglobulin and mucin domain-containing protein 3 (TIM-3). TIM-3 *in vivo* expression was monitored in a metastatic melanoma mouse model using the ⁶⁴Cu-NOTA radiolabeled rat anti-mouse TIM-3-specific monoclonal antibody (RMT3-23) by PET.⁵⁷ A clinical trial investigated the *in vivo* distribution of ¹⁸F-CFA for the reliable monitoring of immune activation post anti-TIM-3 and anti-PD-1 treatment (NCT03409419). However, no results are available to date.

T cell immunoreceptor with Ig and ITIM domains (TIGIT). Two antibody-based TIGIT-specific ⁶⁴Cu- and ⁸⁹Zr-labeled tracers were developed for the preclinical quantification of TIGIT expression on TILs.⁵⁸ These probes could be used to select which patients are candidates for anti-TIGIT immunotherapy.

Imaging other immune cell types

Natural killer (NK) cells. The lack of monitoring and diagnostic platforms to assess of NK-based immunotherapies efficacy has constituted a major drawback to the development of novel therapeutic strategies. NK cells can be imaged in real-time by MRI.⁵⁹ As some iron-oxide nanoparticles have already been approved by the FDA (*e.g.*, ferumoxide, ferumoxytol and ferucarbotran), this approach can be directly translated into the clinic for the short-term monitoring of engineered NK cells. However, nuclear-based imaging remains the most promising methodology for their clinical translation due to the increasing

number of FDA-approved probes.⁵⁹ Notably, Sato *et al* demonstrated that ⁸⁹Zr-oxine labeling of adoptively transferred NK cells from rhesus macaque, here used as a clinically relevant preclinical model, does not impact neither cell phenotype nor viability or function of therapeutic cells, thereby providing a clinically translatable platform for their *in vivo* tracking in humans.⁶⁰

CAR-NK cells. They provide the unique opportunity to engineer off-the-shelf allogeneic products readily available for clinical use. Direct labeling is a readily applicable method to monitor their *in vivo* fate in patients,⁵⁹ whereas the challenges posed by the intrinsic properties of NK cells (*e.g.*, poor transduction with retroviral and lentiviral methods) have delayed the development of an indirect and clinically compatible long-term monitoring tool.

Dendritic cells (DCs). *In vivo* tracking of DCs is typically achieved by direct labeling. Aarntzen *et al* proved that pretreatment of melanoma patients with an extra dose of ¹⁹F-labeled DCs does not improve their relocation to the lymph nodes, a prerequisite for them to trigger an effective immune response.⁶¹ The same author used [¹⁸F]FLT to visualize T and B cell proliferation as a readout of early immune responses after administration of DC vaccine therapy in melanoma patients with lymph nodal metastases (figure 2E; NCT00243594, NCT00243529).⁶² Accuracy of intranodal and internodal delivery and *in vivo* distribution of DCs can be assessed by superparamagnetic iron oxide nanoparticles (SPIONs) MRI (figure 2F).⁶³ A comprehensive list of MRI-based DCs imaging is in overview from Bulte and Shakeri-Zadeh.⁶⁴ Alternatively, DCs can be imaged using reporter genes, including NIS⁶⁵ and ferritin.⁶⁶

Monocytes and macrophages. As highly phagocytic cells, they can efficiently take up SPIONs⁶⁷ and ¹⁹F-PFC⁶⁸ and be monitored by MRI. Tumor-associated macrophages preferentially incorporate the FDA-approved iron oxide nanoparticle compound ferumoxitol and can be preclinically imaged by MRI.⁶⁷ CAR-macrophages (CAR-M)⁶⁹ were pioneered in Gill's laboratory at UPenn and entered the very first in-human phase 1 multicenter clinical trial for the treatment of metastatic HER2-positive solid tumors (NCT04660929). With more of CAR-M being developed, we expect to see an increase of preclinical and clinical testing employing molecular imaging.

Imaging Cellular Immunotherapies: a Future Perspective

With the constant expansion of the cellular immunotherapy arsenal, imaging the *in vivo* fate of cellular immunotherapies is paramount for the reliable assessment and prediction of therapeutic responses. As reporter genes have multiple advantages over the direct labeling approach, they could be fully integrated into clinical practice. The clinical studies involving HSV1-*tk* (figure 2A and table 2) have set the stage for expanding the portfolio of clinically used reporters for cellular immunotherapies imaging. However, some impediments have slowed down the process, including the regulatory concerns of using viral delivery systems to introduce the reporter

into the desired therapeutic cells. Since commercially available CAR-T products are now generated through viral delivery (*e.g.*, the lentiviral-based Kymriah and the retroviral-based Yescarta), the skepticism of using them for the delivery of reporter is no longer justified. In addition, vectors could be rendered even safer by using self-inactivating ‘third generation’ versions currently tested in gene therapy.⁷⁰ To avoid the viral-mediated random positioning of reporter genes into the host genome, safer ways based on gene editing (*e.g.*, ZFPs, TALENs and CRISPR-Cas) are available.⁷¹ The delivery at the same time of both the CAR and the reporter (or reporters) is desired, therefore the construction of GMP-compatible cassettes for the delivery of large payloads is needed. Pairing two different reporters (including an inducible one) would allow the simultaneous *in vivo* assessment of distribution and targeting of cellular immunotherapies with the monitoring of their functional status. However, it would also require the development of clinical imaging protocols specifically tailored to this set up. While they provide good image contrast, xenogenic (*e.g.*, HSV1-*tk*) and synthetic reporters can elicit a host immune response. Although this may not represent an issue for preclinical studies, particularly when heavily immunocompromised mouse models are used, it is indeed a barrier for their full integration into clinical practice. Host reporters are a valid alternative as they are recognized as ‘self’ by the immune system. To this class belong two promising candidates for clinical translation, namely the human sodium iodide symporter (hNIS) and the human norepinephrine transporter (hNET) with their respective clinically compatible radioactive PET probes, [¹⁸F]BF₄⁻ and [¹⁸F]MFBG.¹⁴ The limited endogenous expression, the favorable target-to-background ratio, exquisite detection sensitivity and faster tracer clearance, make NIS a superior reporter for the imaging of cellular immunotherapies. Since NIS tracers do not rely on cyclotron accessibility (*e.g.*, ^{99m}TcO₄⁻, ^{xy}XI) and can be produced by automated synthesis at high molar activities (*e.g.*, ¹⁸F-BF₄⁻), their production is greatly simplified and cost effective, making them broadly available for imaging. Moreover, the short half-life of [¹⁸F]BF₄⁻ greatly facilitates the management of patients in a clinical setting.

As host reporters are endogenously expressed in the human body and are responsible for unfavorable contrast, reporters within this class (*e.g.*, hNIS, hNET, hPSMA) need to be strategically selected depending on the expected distribution of the cell-based immunotherapy and location of the tumor. The human somatostatin receptor subtype 2 (hSSTR2) can be endogenously expressed in several immune cell types, including T cells, and may, therefore, not be suited for the imaging of cellular immunotherapies. With the FDA approval of more compatible probes, we do expect a significant increase in usage of reporters in immunotherapy-related clinical trials, but their full integration into clinical practice is still premature. Direct imaging has, therefore, become the fastest approach for clinical translation. Despite the evident

limitations intrinsic to the methodology, the technological advancement of the total-body PET (with its >40 times higher sensitivity than conventional PET) can be used to extend the tracking time of directly labeled cellular immunotherapies and immune-related biomarkers. Many antibodies targeting immune cell therapeutics or immune biomarkers have been successfully conjugated to imaging probes. Some of them are currently being tested in clinical trials, others will soon reach the same stage. However, the applicability of these probes for the *in vivo* monitoring of cellular immunotherapies and biomarkers will be affected by the pharmacodynamics and pharmacokinetics of the therapeutic compound.

Imaging cellular immunotherapies is already playing a central role in guiding the FDA approval of the next generation of off-the-shelf cell-based immunotherapies and in reliably evaluate response in treated patients. Tumors can respond in a heterogeneous manner to cellular immunotherapy.⁷² Biomarkers and checkpoints expression can be heterogeneous too.⁷³ While biopsies alone may not be able to catch with the same level of precision the complexity of the immune response, the latter can be reliably captured by molecular imaging between patients or within the same patient and, sometimes, within the same tumor lesion. Therefore, the clinical application of molecular imaging is not exclusively limited to the *in vivo* monitoring of therapeutic immune cells and their activation status, but also of immune cell biomarkers as a readout of heterogeneous response to immunotherapy, contributing to the identification of patients most likely to benefit from these therapies and thus avoiding unnecessary side effects and reducing the costs associated with ineffective treatment. The increased number of clinical trials of cell-based immunotherapies employing molecular imaging and the constantly expanding clinically approved portfolio of imaging probes will provide justification toward the consolidation of this tool into clinical practice in the years to come. Moreover, radiomics in becoming increasingly important by offering a large array of prospective biomarkers for the interpretation and even prediction of immunotherapy treatment and unfavorable effects. This predictive value increases when combined to other ‘omics’ and/or artificial intelligence.

SUMMARY

Requisites for the successful molecular imaging of cellular immunotherapies:

- ▶ Absent or limited label dilution on cell division (preserved when using indirect reporter gene strategies).
- ▶ Label retention as a prerequisite for repetitive non-invasive *in vivo* imaging.
- ▶ Labeling strategy and imaging probe should not compromise viability, metabolism and/or function of immune cell therapeutics.

Essential requisites for clinical translation:

- ▶ Exquisite sensitivity of the imaging modality (depth penetration) and quantification.
- ▶ Availability of clinically compatible imaging probes.
- ▶ Lack of reporter gene immunogenicity.

Contributors Conceptualization: AV and VP. Writing original draft: AV. Review and editing: AV, VP, PSA and HS.

Funding AV is supported by the EIO Fellowship Award from the Center for Experimental Immuno-Oncology (FP00001443) and the Tow Foundation Fellowship Award (FP00004141) at Memorial Sloan Kettering Cancer Center. VP's laboratory work is supported by NIH Grants (R01 CA220524-01A1, R01 CA204924 and R21 CA250478). PSA's laboratory work is supported by NIH Grants (P30 CA008748, R01 CA236615-01, and R01 CA235667), the U.S. Department of Defense (CA180889 and CA200437), the Mr William H. Goodwin and Alice Goodwin, the Commonwealth Foundation for Cancer Research, and the Experimental Therapeutics Center of Memorial Sloan Kettering Cancer Center. The authors received further support from the NIH/NCI Cancer Center Support Grant to MSKCC (P30 CA008748).

Competing interests Dr Adusumilli declares research funding from ATARA Biotherapeutics, has served on the Scientific Advisory Board or as a consultant to ATARA Biotherapeutics, Bayer, BioArdis, Carisma Therapeutics, Imugene, ImmPACT Bio, and Johnson & Johnson, and has patents, royalties, and intellectual property on mesothelin-targeted CARs and T-cell therapies. Memorial Sloan Kettering Cancer Center has licensed intellectual property related to mesothelin-targeted CARs and T-cell therapies to ATARA Biotherapeutics and has associated financial interests.

Patient consent for publication Not applicable.

Provenance and peer review Commissioned; externally peer reviewed.

Open access This is an open access article distributed in accordance with the Creative Commons Attribution Non Commercial (CC BY-NC 4.0) license, which permits others to distribute, remix, adapt, build upon this work non-commercially, and license their derivative works on different terms, provided the original work is properly cited, appropriate credit is given, any changes made indicated, and the use is non-commercial. See <http://creativecommons.org/licenses/by-nc/4.0/>.

ORCID iDs

Alessia Volpe <http://orcid.org/0000-0003-3087-9178>

Vladimir Ponomarev <http://orcid.org/0000-0002-9119-9128>

REFERENCES

- 1 Kircher MF, Gambhir SS, Grimm J. Noninvasive cell-tracking methods. *Nat Rev Clin Oncol* 2011;8:677–88.
- 2 Blasberg RG, Gelovani J. Molecular-genetic imaging: a nuclear medicine-based perspective. *Mol Imaging* 2002;1:280–300.
- 3 Serganova I, Blasberg RG. Molecular imaging with reporter genes: has its promise been delivered? *J Nucl Med* 2019;60:1665–81.
- 4 Rivera-Rodriguez A, Hoang-Minh LB, Chiu-Lam A, et al. Tracking adoptive T cell immunotherapy using magnetic particle imaging. *Nanotheranostics* 2021;5:431–44.
- 5 Graves EE, Weissleder R, Ntziachristos V. Fluorescence molecular imaging of small animal tumor models. *Curr Mol Med* 2004;4:419–30.
- 6 Volpe A, Kurtys E, Fruhwirth GO. Cousins at work: how combining medical with optical imaging enhances in vivo cell tracking. *Int J Biochem Cell Biol* 2018;102:40–50.
- 7 Mezzanotte L, van 't Root M, Karatas H, et al. In vivo molecular bioluminescence imaging: new tools and applications. *Trends Biotechnol* 2017;35:640–52.
- 8 Wu Y, Liu Y, Huang Z, et al. Control of the activity of CAR-T cells within tumours via focused ultrasound. *Nat Biomed Eng* 2021;5:1336–47.
- 9 Farhadi A, Ho GH, Sawyer DP, et al. Ultrasound imaging of gene expression in mammalian cells. *Science* 2019;365:1469–75.
- 10 Bulte JWM, Kraitchman DL. Iron oxide MR contrast agents for molecular and cellular imaging. *NMR Biomed* 2004;17:484–99.
- 11 Gilad AA, Ziv K, McMahon MT, et al. MR reporter genes. *J Nucl Med* 2008;49:1905–8.
- 12 Bulte JWM, Daldrop-Link HE. Clinical tracking of cell transfer and cell transplantation: trials and tribulations. *Radiology* 2018;289:604–15.
- 13 Haris M, Bagga P, Hariharan H, et al. Molecular imaging biomarkers for cell-based immunotherapies. *J Transl Med* 2017;15:140.
- 14 Volpe A, Pillarsetty NVK, Lewis JS, et al. Applications of nuclear-based imaging in gene and cell therapy: probe considerations. *Mol Ther Oncolytics* 2021;20:447–58.
- 15 Sato N, Wu H, Asiedu KO, et al. (89)Zr-Oxine Complex PET Cell Imaging in Monitoring Cell-based Therapies. *Radiology* 2015;275:490–500.
- 16 Pittet MJ, Grimm J, Berger CR, et al. In vivo imaging of T cell delivery to tumors after adoptive transfer therapy. *Proc Natl Acad Sci U S A* 2007;104:12457–61.
- 17 Massicano AVF, Bartels JL, Jeffers CD. Production of [(89)Zr] Oxinate(4) and cell radiolabeling for human use. *J Labelled Comp Radiopharm* 2021;64:209–16.
- 18 Costa GL, Sandora MR, Nakajima A, et al. Adoptive immunotherapy of experimental autoimmune encephalomyelitis via T cell delivery of the IL-12 p40 subunit. *J Immunol* 2001;167:2379–87.
- 19 Rabinovich BA, Ye Y, Etto T, et al. Visualizing fewer than 10 mouse T cells with an enhanced firefly luciferase in immunocompetent mouse models of cancer. *Proc Natl Acad Sci U S A* 2008;105:14342–6.
- 20 Koehne G, Doubrovin M, Doubrovina E, et al. Serial in vivo imaging of the targeted migration of human HSV-TK-transduced antigen-specific lymphocytes. *Nat Biotechnol* 2003;21:405–13.
- 21 Borst J, Ahrends T, Bąbala N, et al. CD4⁺ T cell help in cancer immunology and immunotherapy. *Nat Rev Immunol* 2018;18:635–47.
- 22 Doubrovin MM, Doubrovina ES, Zanzonico P, et al. In vivo imaging and quantitation of adoptively transferred human antigen-specific T cells transduced to express a human norepinephrine transporter gene. *Cancer Res* 2007;67:11959–69.
- 23 Kenanova V, Barat B, Olafsen T, et al. Recombinant carcinoembryonic antigen as a reporter gene for molecular imaging. *Eur J Nucl Med Mol Imaging* 2009;36:104–14.
- 24 Weist MR, Starr R, Aguilar B, et al. PET of Adoptively Transferred Chimeric Antigen Receptor T Cells with ⁸⁹Zr-Oxine. *J Nucl Med* 2018;59:1531–7.
- 25 Lee SH, Soh H, Chung JH, et al. Feasibility of real-time in vivo ⁸⁹Zr-DFO-labeled CAR T-cell trafficking using PET imaging. *PLoS One* 2020;15:e0223814.
- 26 Moroz MA, Zhang H, Lee J, et al. Comparative analysis of T cell imaging with human nuclear reporter genes. *J Nucl Med* 2015;56:1055–60.
- 27 Volpe A, Lang C, Lim L, et al. Spatiotemporal PET imaging reveals differences in CAR-T tumor retention in triple-negative breast cancer models. *Mol Ther* 2020;28:2271–85.
- 28 Minn I, Huss DJ, Ahn H-H, et al. Imaging CAR T cell therapy with PSMA-targeted positron emission tomography. *Sci Adv* 2019;5:eaaw5096.
- 29 Sellmyer MA, Richman SA, Lohith K, et al. Imaging CAR T cell trafficking with eDHFR as a PET reporter gene. *Mol Ther* 2020;28:42–51.
- 30 Krebs S, Ahad A, Carter LM, et al. Antibody with infinite affinity for in vivo tracking of genetically engineered lymphocytes. *J Nucl Med* 2018;59:1894–900.
- 31 Keu KV, Witney TH, Yaghoubi S, et al. Reporter gene imaging of targeted T cell immunotherapy in recurrent glioma. *Sci Transl Med* 2017;9. doi:10.1126/scitranslmed.aag2196. [Epub ahead of print: 18 01 2017].
- 32 Mohseni YR, Tung SL, Dudreuilh C, et al. The future of regulatory T cell therapy: promises and challenges of implementing CAR technology. *Front Immunol* 2020;11:1608. doi:10.3389/fimmu.2020.01608
- 33 Jacob J, Nadkarni S, Volpe A, et al. Spatiotemporal in vivo tracking of polyclonal human regulatory T cells (Tregs) reveals a role for innate immune cells in Treg transplant recruitment. *Mol Ther Methods Clin Dev* 2021;20:324–36.
- 34 Mohseni YR, Saleem A, Tung SL, et al. Chimeric antigen receptor-modified human regulatory T cells that constitutively express IL-10 maintain their phenotype and are potently suppressive. *Eur J Immunol* 2021;51:2522–30.
- 35 Man F, Lim L, Volpe A, et al. In Vivo PET Tracking of ⁸⁹Zr-Labeled Vγ9Vδ2 T Cells to Mouse Xenograft Breast Tumors Activated with Liposomal Alendronate. *Mol Ther* 2019;27:219–29.
- 36 van de Donk PP, Kist de Ruijter L, Lub-de Hooge MN, et al. Molecular imaging biomarkers for immune checkpoint inhibitor therapy. *Theranostics* 2020;10:1708–18.
- 37 van de Donk PP, Wind TT, Hooiveld-Noeken JS, et al. Interleukin-2 PET imaging in patients with metastatic melanoma before and during immune checkpoint inhibitor therapy. *Eur J Nucl Med Mol Imaging* 2021;48:4369–76.

- 38 Tavaré R, Escuin-Ordinas H, Mok S, *et al.* An effective Immuno-PET imaging method to monitor CD8-Dependent responses to immunotherapy. *Cancer Res* 2016;76:73–82.
- 39 Pandit-Taskar N, Postow MA, Hellmann MD, *et al.* First-in-Humans Imaging with ⁸⁹Zr-Df-IAB2M2C Anti-CD8 Minibody in Patients with Solid Malignancies: Preliminary Pharmacokinetics, Biodistribution, and Lesion Targeting. *J Nucl Med* 2020;61:512–9.
- 40 Fredriksson F, Tavaré R, Giurleo J. Evaluation of ⁸⁹Zr-labeled Anti-CD8 Fully Human Monoclonal Antibody REGN5054 in Cynomolgus Monkeys. *Journal of Nuclear Medicine* 2020;61:158–58.
- 41 Larimer BM, Wehrenberg-Klee E, Dubois F, *et al.* Granzyme B PET imaging as a predictive biomarker of immunotherapy response. *Cancer Res* 2017;77:2318–27.
- 42 Gibson HM, McKnight BN, Malysa A, *et al.* Ifn γ PET imaging as a predictive tool for monitoring response to tumor immunotherapy. *Cancer Res* 2018;78:5706–17.
- 43 Ponomarev V, Doubrovin M, Lyddane C, *et al.* Imaging TCR-dependent NFAT-mediated T-cell activation with positron emission tomography in vivo. *Neoplasia* 2001;3:480–8.
- 44 Hooijberg E, Bakker AQ, Ruizendaal JJ, *et al.* NFAT-controlled expression of GFP permits visualization and isolation of antigen-stimulated primary human T cells. *Blood* 2000;96:459–66.
- 45 Na I-K, Markley JC, Tsai JJ, *et al.* Concurrent visualization of trafficking, expansion, and activation of T lymphocytes and T-cell precursors in vivo. *Blood* 2010;116:e18–25.
- 46 van der Veen EL, Bensch F, Glaudemans AWJM, *et al.* Molecular imaging to enlighten cancer immunotherapies and underlying involved processes. *Cancer Treat Rev* 2018;70:232–44.
- 47 England CG, Ehlerding EB, Hernandez R, *et al.* Preclinical pharmacokinetics and biodistribution studies of ⁸⁹Zr-labeled pembrolizumab. *J Nucl Med* 2017;58:162–8.
- 48 England CG, Jiang D, Ehlerding EB, *et al.* ⁸⁹Zr-labeled nivolumab for imaging of T-cell infiltration in a humanized murine model of lung cancer. *Eur J Nucl Med Mol Imaging* 2018;45:110–20.
- 49 Kok IC, Hooiveld JS, van de Donk PP, *et al.* ⁸⁹Zr-pembrolizumab imaging as a non-invasive approach to assess clinical response to PD-1 blockade in cancer. *Ann Oncol* 2022;33:80–8.
- 50 Broos K, Keyaerts M, Lecocq Q, *et al.* Non-Invasive assessment of murine PD-L1 levels in syngeneic tumor models by nuclear imaging with nanobody tracers. *Oncotarget* 2017;8:41932–46.
- 51 Donnelly DJ, Smith RA, Morin P, *et al.* Synthesis and Biologic Evaluation of a Novel ¹⁸F-Labeled Adnectin as a PET Radioligand for Imaging PD-L1 Expression. *J Nucl Med* 2018;59:529–35.
- 52 Ehlerding EB, England CG, Majewski RL, *et al.* ImmunoPET imaging of CTLA-4 expression in mouse models of non-small cell lung cancer. *Mol Pharm* 2017;14:1782–9.
- 53 Ehlerding EB, Lee HJ, Jiang D, *et al.* Antibody and fragment-based PET imaging of CTLA-4+ T-cells in humanized mouse models. *Am J Cancer Res* 2019;9:53–63.
- 54 Ribas A, Benz MR, Allen-Auerbach MS, *et al.* Imaging of CTLA4 blockade-induced cell replication with (18)F-FLT PET in patients with advanced melanoma treated with tremelimumab. *J Nucl Med* 2010;51:340–6.
- 55 Lecocq Q, Zeven K, De Vlaeminck Y, *et al.* Noninvasive imaging of the immune checkpoint LAG-3 using nanobodies, from development to pre-clinical use. *Biomolecules* 2019;9. doi:10.3390/biom9100548. [Epub ahead of print: 29 09 2019].
- 56 Kelly MP, Tavaré R, Giurleo J. Abstract 3033: Immuno-PET detection of LAG-3 expressing intratumoral lymphocytes using the zirconium-89 radiolabeled fully human anti-LAG-3 antibody REGN3767. *Cancer Res* 2018;78:3033–33.
- 57 Wei W, Jiang D, Lee HJ, *et al.* ImmunoPET imaging of Tim-3 in murine melanoma models. *Adv Ther* 2020;3. doi:10.1002/adtp.202000018. [Epub ahead of print: 17 04 2020].
- 58 Shaffer T, Natarajan A, Gambhir SS. Pet imaging of TIGIT expression on tumor-infiltrating lymphocytes. *Clin Cancer Res* 2021;27:1932–40.
- 59 Varani M, Auletta S, Signore A, *et al.* State of the art of natural killer cell imaging: a systematic review. *Cancers* 2019;11. doi:10.3390/cancers11070967. [Epub ahead of print: 09 07 2019].
- 60 Sato N, Stringaris K, Davidson-Moncada JK, *et al.* In Vivo Tracking of Adoptively Transferred Natural Killer Cells in Rhesus Macaques Using ⁸⁹Zirconium-Oxine Cell Labeling and PET Imaging. *Clin Cancer Res* 2020;26:2573–81.
- 61 Aarntzen EHJG, Srinivas M, Bonetto F, *et al.* Targeting of 111In-labeled dendritic cell human vaccines improved by reducing number of cells. *Clin Cancer Res* 2013;19:1525–33.
- 62 Aarntzen EHJG, Srinivas M, De Wilt JHW, *et al.* Early identification of antigen-specific immune responses in vivo by [18F]-labeled 3'-fluoro-3'-deoxy-thymidine ([18F]FLT) PET imaging. *Proc Natl Acad Sci U S A* 2011;108:18396–9.
- 63 de Vries IJM, Lesterhuis WJ, Barentsz JO, *et al.* Magnetic resonance tracking of dendritic cells in melanoma patients for monitoring of cellular therapy. *Nat Biotechnol* 2005;23:1407–13.
- 64 Bulte JWM, Shakeri-Zadeh A. In vivo MRI tracking of tumor vaccination and antigen presentation by dendritic cells. *Mol Imaging Biol* 2022;24:1–10.
- 65 Lee SB, Lee HW, Lee H, *et al.* Tracking dendritic cell migration into lymph nodes by using a novel PET probe ¹⁸F-tetrafluoroborate for sodium/iodide symporter. *EJNMMI Res* 2017;7:32.
- 66 Kim HS, Woo J, Lee JH, *et al.* In vivo tracking of dendritic cell using MRI reporter gene, ferritin. *PLoS One* 2015;10:e0125291.
- 67 Daldrup-Link HE, Golovko D, Ruffell B, *et al.* MRI of tumor-associated macrophages with clinically applicable iron oxide nanoparticles. *Clin Cancer Res* 2011;17:5695–704.
- 68 Fink C, Gaudet JM, Fox MS, *et al.* ¹⁹F-perfluorocarbon-labeled human peripheral blood mononuclear cells can be detected in vivo using clinical MRI parameters in a therapeutic cell setting. *Sci Rep* 2018;8:590.
- 69 Klichinsky M, Ruella M, Shestova O, *et al.* Human chimeric antigen receptor macrophages for cancer immunotherapy. *Nat Biotechnol* 2020;38:947–53.
- 70 Milone MC, O'Doherty U. Clinical use of lentiviral vectors. *Leukemia* 2018;32:1529–41.
- 71 Ashmore-Harris C, Fruhwirth GO. The clinical potential of gene editing as a tool to engineer cell-based therapeutics. *Clin Transl Med* 2020;9:15.
- 72 Majzner RG, Ramakrishna S, Yeom KW, *et al.* GD2-CAR T cell therapy for H3K27M-mutated diffuse midline gliomas. *Nature* 2022;603:934–41. doi:10.1038/s41586-022-04489-4
- 73 Mansfield AS, Murphy SJ, Peikert T, *et al.* Heterogeneity of programmed cell death ligand 1 expression in multifocal lung cancer. *Clin Cancer Res* 2016;22:2177–82.
- 74 Skovgard MS, Hocine HR, Saini JK, *et al.* Imaging CAR T-cell kinetics in solid tumors: translational implications. *Mol Ther Oncolytics* 2021;22:355–67.
- 75 Hingorani DV, Chapelin F, Stares E, *et al.* Cell penetrating peptide functionalized perfluorocarbon nanoemulsions for targeted cell labeling and enhanced fluorine-19 MRI detection. *Magn Reson Med* 2020;83:974–87.
- 76 Simonetta F, Alam IS, Lohmeyer JK, *et al.* Molecular imaging of chimeric antigen receptor T cells by ICOS-ImmunoPET. *Clin Cancer Res* 2021;27:1058–68.
- 77 Alam IS, Simonetta F, Scheller L, *et al.* Visualization of activated T cells by OX40-ImmunoPET as a strategy for diagnosis of acute graft-versus-host disease. *Cancer Res* 2020;80:4780–90.
- 78 Hartimath SV, Draghiciu O, van de Wall S, *et al.* Noninvasive monitoring of cancer therapy induced activated T cells using [¹⁸F]FB-IL-2 PET imaging. *Oncoimmunology* 2017;6:e1248014.
- 79 Griessinger CM, Maurer A, Kesenheimer C, *et al.* ⁶⁴Cu antibody-targeting of the T-cell receptor and subsequent internalization enables in vivo tracking of lymphocytes by PET. *Proc Natl Acad Sci U S A* 2015;112:1161–6.
- 80 Beckford Vera DR, Smith CC, Bixby LM, *et al.* Immuno-PET imaging of tumor-infiltrating lymphocytes using zirconium-89 radiolabeled anti-CD3 antibody in immune-competent mice bearing syngeneic tumors. *PLoS One* 2018;13:e0193832.
- 81 Larimer BM, Wehrenberg-Klee E, Caraballo A, *et al.* Quantitative CD3 PET imaging predicts tumor growth response to anti-CTLA-4 therapy. *J Nucl Med* 2016;57:1607–11.
- 82 Freise AC, Zettlitz KA, Salazar FB, *et al.* ImmunoPET imaging of murine CD4+ T cells using anti-CD4 Cys-Diabody: effects of protein dose on T cell function and imaging. *Mol Imaging Biol* 2017;19:599–609. doi:10.1007/s11307-016-1032-z
- 83 Seo JW, Tavaré R, Mahakian LM, *et al.* CD8+ T-Cell Density Imaging with ⁶⁴Cu-Labeled Cys-Diabody Informs Immunotherapy Protocols. *Clin Cancer Res* 2018;24:4976–87.
- 84 Kircher MF, Allport JR, Graves EE, *et al.* In vivo high resolution three-dimensional imaging of antigen-specific cytotoxic T-lymphocyte trafficking to tumors. *Cancer Res* 2003;63:6838–46.
- 85 Levi J, Goth S, Huynh L, *et al.* ¹⁸F-AraG PET for CD8 Profiling of Tumors and Assessment of Immunomodulation by Chemotherapy. *J Nucl Med* 2021;62:802–807.
- 86 Schwarzenberg J, Radu CG, Benz M, *et al.* Human biodistribution and radiation dosimetry of novel PET probes targeting the deoxyribonucleoside salvage pathway. *Eur J Nucl Med Mol Imaging* 2011;38:711–21.
- 87 Kim W, Le TM, Wei L, *et al.* [18F]CFA as a clinically translatable probe for PET imaging of deoxycytidine kinase activity. *Proc Natl Acad Sci U S A* 2016;113:4027–32.



- 88 Natarajan A, Mayer AT, Xu L, *et al.* Novel radiotracer for ImmunoPET imaging of PD-1 checkpoint expression on tumor infiltrating lymphocytes. *Bioconjug Chem* 2015;26:2062–9.
- 89 Hettich M, Braun F, Bartholomä MD, *et al.* High-Resolution PET imaging with therapeutic antibody-based PD-1/PD-L1 checkpoint tracers. *Theranostics* 2016;6:1629–40.
- 90 Lameijer M, Binderup T, van Leent MMT, *et al.* Efficacy and safety assessment of a TRAF6-targeted nanoimmunotherapy in atherosclerotic mice and non-human primates. *Nat Biomed Eng* 2018;2:279–92.
- 91 Markovic SN, Galli F, Suman VJ, *et al.* Non-invasive visualization of tumor infiltrating lymphocytes in patients with metastatic melanoma undergoing immune checkpoint inhibitor therapy: a pilot study. *Oncotarget* 2018;9:30268–78.
- 92 de Ruijter LK, van de Donk PP, Hooiveld-Noeken JS. Abstract LB037: ⁸⁹ZED88082A PET imaging to visualize CD8⁺ T cells in patients with cancer treated with immune checkpoint inhibitor. *Cancer Res* 2021;81:LB037–LB37.
- 93 Namavari M, Chang Y-F, Kusler B, *et al.* Synthesis of 2'-deoxy-2'-[18F]fluoro-9-β-D-arabinofuranosylguanine: a novel agent for imaging T-cell activation with PET. *Mol Imaging Biol* 2011;13:812–8. doi:10.1007/s11307-010-0414-x
- 94 Ponomarev V. Advancing immune and cell-based therapies through imaging. *Mol Imaging Biol* 2017;19:379–84.
- 95 Lecocq Q, Keyaerts M, Devoogdt N. The Next-Generation Immune Checkpoint LAG-3 and Its Therapeutic Potential in Oncology: Third Time's a Charm. *International Journal of Molecular Sciences* 2022;22:1.
- 96 Barrio MJ, Spick C, Radu CG, *et al.* Human Biodistribution and Radiation Dosimetry of ¹⁸F-Clofarabine, a PET Probe Targeting the Deoxyribonucleoside Salvage Pathway. *J Nucl Med* 2017;58:374–8.
- 97 Slovin SF, Wang X, Hullings M, *et al.* Chimeric antigen receptor (CAR⁺) modified T cells targeting prostate-specific membrane antigen (PSMA) in patients (PTS) with castrate metastatic prostate cancer (CMPC). *Journal of Clinical Oncology* 2013;31:72.
- 98 Eissenberg LG, Rettig MP, Ritchey JK, *et al.* [(18)F]FHBG PET/CT Imaging of CD34-TK75 Transduced Donor T Cells in Relapsed Allogeneic Stem Cell Transplant Patients: Safety and Feasibility. *Mol Ther* 2015;23:1110–22.
- 99 Krekorian M, Fruhwirth GO, Srinivas M, *et al.* Imaging of T-cells and their responses during anti-cancer immunotherapy. *Theranostics* 2019;9:7924–47.
- 100 Bensch F, van der Veen EL, Lub-de Hooge MN, *et al.* ⁸⁹Zr-atezolizumab imaging as a non-invasive approach to assess clinical response to PD-L1 blockade in cancer. *Nat Med* 2018;24:1852–8.